

# MULTI-SCALE COLLABORATIVE SEARCHING THROUGH SWARMING

Wangyi Liu, Yasser E. Taima, Martin B. Short, Andrea L. Bertozzi  
*Department of Mathematics, University of California, Los Angeles, CA 90095-1555, U.S.A. \**  
{bobbyliu, ytaima, mbshort, bertozzi}@math.ucla.edu

Keywords: Mobile Robots, Autonomous Agents, Searching, Swarming, Target Detection.

Abstract: This paper presents a multi-scale searching and target-locating algorithm for a group of agents moving in a swarm and sensing potential targets. The aim of the algorithm is to use these agents to efficiently search for and locate targets with a finite sensing radius in some bounded area. We present an algorithm that both controls agent movement and analyzes sensor signals to determine where targets are located. We use computer simulations to determine the effectiveness of this collaborative searching. We derive some physical scaling properties of the system and compare the results to the data from the simulations.

## 1 INTRODUCTION

Collaborative sensing has long attracted research interest. Researchers have investigated scenarios where sensors require localization (Bullo and Cortes, 2005), where they are used to control collaborative movement (Bopardikar et al., 2007), detect a scalar field (Gao et al., 2008), or perform a collaborative task (Smith and Bullo, 2009). Using such collaborating sensors to detect and locate targets within an area has been studied in reference to the “mine counter-measure” problem (Cook et al., 2003), the specific military task of locating ground or water-based mines.

In this paper, we develop a multi-scale search and target-locating algorithm for a type of mine counter-measure problem in which a number of independent agents are given the task of determining the precise location of targets within a domain. The algorithm is designed to handle problems where the scale of the target sensing radius is much smaller than the domain size. The focus of this work is to identify optimality of the algorithm as a function of the swarm size, the number of agents per group and the distribution of resources into different groups.

We assume a simply-connected domain, and use

---

\*This paper is supported by ARO MURI grant 50363-MA-MUR, ONR grant N000141010641 and NSF grant DMS-0914856.

noisy sensors that detect a scalar quantity emitted by each target, but only when an agent is within a fixed distance  $r_s$  from a target. We control the motion of the agents with a model that makes the individuals form distinct swarms, and present filtering techniques that allow for locating targets despite noisy data. The inspiration for this approach comes in part from biology, as in the example of birds forming flocks when flying and searching for food (Travis, 2007).

Next, we analytically derive some of the system’s main scaling properties, such as the relationship between swarm size, distance between agents and target sensing radius, and compare with the experimentally recorded data. We conclude that our analytical approach matches well the data from the simulations.

We assume a sensing radius  $r_s$  much smaller than the domain but comparable to or less than the swarm size. Other assumptions, however, may require different algorithms. For example, in (Burger et al., 2008) the sensing radius is infinite, but sensing is limited by obstacles, and in (Olfati-Saber, 2007) communication between agents is not always possible.

### 1.1 Scenario Description

We consider  $M$  targets in a two-dimensional simply-connected domain, that is, a flat enclosed area with no holes, and  $N$  agents able to move freely within

the domain. Each target emits a radially symmetric scalar signal  $g(r)$  that decays with the distance  $r$  from the target, and drops to zero at some  $r_s$ , the target’s sensing radius. Agents detect this signal with an additional Gaussian, scalar white noise component added. If an agent is within the sensing radius of multiple targets, it detects only the sum of the individual signals, again with a noise component added. We suppose that an agent takes sensor readings at regular intervals (once per “time step”) spaced such that the noise between time steps can be assumed independent.

The algorithm accomplishes 3 tasks: it filters the noisy sensor data, controls the coordinated movement of the agents based on this data, and determines when a target has been acquired and where it is located.

## 1.2 Structure of the Paper

The algorithm is described in the next three sections: Section 2 focuses on the techniques we use to process sensor data, Section 3 describes the movement control of the agents, and Section 4 describes the method for locating a target. The algorithm is evaluated in Section 5. Scaling properties are derived and checked against simulations in Section 6, followed by a conclusion and ideas for future research in Section 7.

## 2 SENSOR DATA PROCESSING

Due to noise in the agent sensor readings and the sensing radius  $r_s$  being finite, we employ two distinct filters to the data from the readings: a Kalman filter and a Cumulative Sum (CUSUM) filter. The Kalman filter reduces or eliminates the noise in the data, while the CUSUM filter is well-suited to determining whether or not an agent is within the sensing radius of a target. The sensor data model follows as a mathematical formula. As explained in Section 1, the formula describes sensor readings as the sum of scalar signals that depend only on the distance from a target, together with a noise component.

Given the  $M$  targets at positions  $y_j$  and an agent  $i$  with current position  $x_i(t_k)$  at timestep  $k$ , the agent sensor reading  $s_i(t_k)$  is given by

$$s_i(t_k) = \sum_{j=1}^M g(|y_j - x_i(t_k)|) + n_i(t_k), \quad (1)$$

where  $n_i(t_k)$  denotes sensor noise and  $g(r)$  is the signal strength at a distance  $r$  from the target. For simplicity, we assume  $g(r)$  is isotropic, smooth, decaying, the same for all targets, and has a cutoff at  $r_s$ .

## 2.1 Kalman Filtering

Before using the agent sensor readings to locate targets or control agent motion, we pass the sensor readings through a Kalman filter. Since the signal from the target is presumed to be varying smoothly with the distance to the target  $r$  (up to the cutoff point  $r_s$ ) as the agents navigate the environment, a Kalman filter is a natural choice to eliminate or reduce noise in the sensor readings. The Kalman filter takes the sensor reading  $s_i(t_k)$  of agent  $i$  at time  $t_k$ , and converts it into the filtered data  $f_i(t_k)$  according to

$$P_i(t_k) = \frac{P_i(t_{k-1})R_i(t_k)}{P_i(t_{k-1}) + R_i(t_k)} + Q_i(t_k), \quad (2)$$

and

$$f_i(t_k) = f_i(t_{k-1}) + \frac{P_i(t_k)(s_i(t_k) - f_i(t_{k-1}))}{P_i(t_k) + R_i(t_k)}. \quad (3)$$

Here  $R_i(t_k)$  is the square of the noise amplitude, known or estimated by the agent, and  $Q_i(t_k)$  is the square of the change of the signal amplitude between two time steps, either fixed beforehand or estimated using the current velocity of the agent (in this paper, it is fixed beforehand).  $P_i(t_k)$  is roughly the variance of the sensor reading’s amplitude. The output  $f_i(t_k)$  of this filter is then used in target-locating, as described in Section 4.

## 2.2 Threshold Check and the CUSUM Filter

Before attempting to locate targets, an agent needs to determine whether or not it is receiving an actual signal, rather than just noise. In other words, an agent needs to determine whether it is within the sensing radius of a target at each time-step  $t_k$ . This information is then used both in controlling the movement of the agents and in determining when to begin estimating a target’s position. In order to determine the sensing status of an individual agent, we employ a CUSUM filter, as this type of filter is well-suited to determining abrupt changes of state (Page, 1954), and has been used in the similar task of boundary tracking (Jin and Bertozzi, 2007; Chen et al., 2009). The filter keeps a sort of running average of the signal and notes when this average seems to have risen above a certain threshold, indicating that the agent is now within the sensing radius of a target. As the noise is effectively summed up by the filter, it tends to cancel out.

In the original form of the CUSUM filter, we imagine a sensor that returns a sequence of independent observations  $s(t_1) \dots s(t_n)$ , each of which follows one of two probability density functions: a pre-change function  $g_0$  and a post-change function  $g_1$ .

The log-likelihood ratio is

$$Z(t_k) = \log[g_1(s(t_k))/g_0(s(t_k))], \quad (4)$$

and we define the CUSUM statistic as

$$U(t_k) = \max(0, Z(t_k) + U(t_{k-1})), \quad U(t_0) = 0. \quad (5)$$

We then choose a threshold  $\bar{U}$ , and when  $U(t_k) \geq \bar{U}$  for the first time, the algorithm ends and we declare that the state has changed from  $g_0$  to  $g_1$ . The threshold should be chosen so as to minimize both false-alarms (these happen more frequently for small  $\bar{U}$ ) and time to detection (this gets larger as  $\bar{U}$  increases).

In our system, we choose the special case where sensor reading follows a Gaussian distribution. In the pre-change state  $g_0$ , the agent is outside the sensing radius of any target and reads only noise, which we model as a Gaussian with zero mean and variance  $\sigma^2$ . In the post-change state  $g_1$ , the agent enters the sensing radius of a target, and although the probability distribution is still a Gaussian with the same variance, the mean is now larger than zero, which we set to be  $2B$ . Then

$$\begin{aligned} Z(t_k) &= \log \left[ \frac{e^{-[s(t_k)-2B]^2/2\sigma^2}/(\sigma\sqrt{2\pi})}{e^{-s(t_k)^2/2\sigma^2}/(\sigma\sqrt{2\pi})} \right] \\ &= \frac{-[s(t_k) - 2B]^2}{2\sigma^2} + \frac{s(t_k)^2}{2\sigma^2} \\ &= \frac{2B}{\sigma^2} [s(t_k) - B]. \end{aligned} \quad (6)$$

We also modify the algorithm so that it can detect status changes both into and out of detection zones. Thus, we implement two filter values:  $U_i(t_k)$  to determine when an agent has entered a zone, and  $L_i(t_k)$  to determine if it has left a zone. We also define a binary function  $b_i(t_k)$  which denotes the status of an agent:  $b_i(t_k) = 1$  means that the agent is near a target and  $b_i(t_k) = 0$  means otherwise. The filter values all start at zero, and are thus updated according to

$$U_i(t_k) = \max(0, s_i(t_k) - B + U_i(t_{k-1})), \quad (7)$$

$$L_i(t_k) = \min(0, s_i(t_k) - B + L_i(t_{k-1})), \quad (8)$$

and

$$b_i(t_k) = \begin{cases} 1 & b_i(t_{k-1}) = 0, U_i(t_k) > \bar{U} \\ 0 & b_i(t_{k-1}) = 1, L_i(t_k) < \bar{L} \\ b_i(t_{k-1}) & \text{otherwise.} \end{cases} \quad (9)$$

In addition, when the status of agent  $i$  changes, we reset the corresponding  $U_i$  or  $L_i$  to zero. Lastly, we have set the constant coefficient  $\frac{2B}{\sigma^2} = 1$  for convenience.

Recall that  $B$  is a sensor value that is less than the predicted mean when inside a sensing radius, and  $\bar{U}$  is our chosen detection threshold. So, when the agent is near a target, the sensor reading  $s_i(t_k)$  tends to be

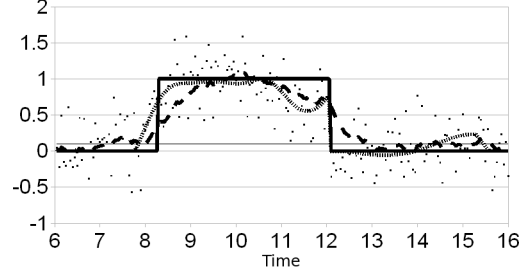


Figure 1: Example filter output for an agent as a function of time, from one of our simulations. The densely-dotted line represents the true signal that ought to be detected by the agent. The dots are the actual noisy signal detected by the agent (i.e., the densely-dotted curve plus noise). The thicker step function is the signal status returned by the CUSUM filter, and the thinner straight line represents the value  $B = 0.1$ . The sparsely-dashed curve is the output of the Kalman filter when applied to the detected noisy signal.

larger than  $B$ , causing  $U_i(t_k)$  to grow quickly until it is larger than  $\bar{U}$ , indicating a change in status. The converse is true if an agent leaves the sensing region of a target. The values of filter parameters,  $\bar{U}$ ,  $\bar{L}$  and  $B$  are problem-specific, and should be set in a manner that minimizes false-alarms while keeping the average time to detection as low as possible, as mentioned above.

An example of sensor reading for an agent from one of our simulations is in Fig. 1. The Kalman filter does a good job of reducing noise, bringing the sensor readings much closer to the true signal. Near the middle of the plot, the agent enters into the sensing radius of a target; this is reflected by a transition within the CUSUM filter from  $b = 0$  to  $b = 1$ . There is, as expected from the behavior of CUSUM, a slight delay between when the agent actually enters into the radius and when this transition of  $b$  occurs. After spending some time within the sensing radius, the estimated target location stabilizes, the agent subtracts the true signal from its measurements (this will be explained in Section 4), and the agent leaves to find further targets.

### 3 AGENT MOVEMENT CONTROL

We have chosen to control the movement of our agents by breaking up our total agent population  $N$  into a number of distinct, leaderless “swarms”. This is done for a variety of reasons. Firstly, it increases robustness, as any individual swarm member is not critical to the functioning of the swarm as a whole.

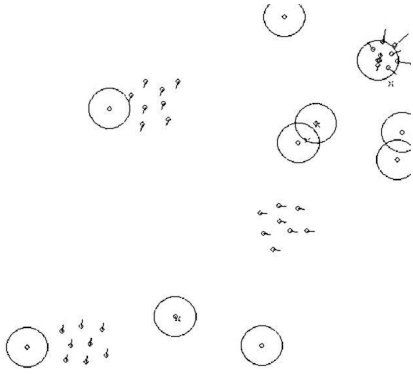


Figure 2: A screenshot from the simulation. Four swarms with eight agents each are used. Three of them are in the searching phase, and the upper right swarm is in the target-locating phase. The large circle around each target marks the sensing radius. Small crosses are already located targets.

Secondly, since we imagine that any sensor data acquired by readings from the agents is local in space, a swarm provides a method of extending the effective sensing zone to the whole swarm. Thirdly, a swarm of nearby agents may use their combined measurements to decrease sensor noise. Finally, a swarm provides the ability to locate targets via triangulation or gradient methods. Each swarm may search within its designated region of space if a divide-and-conquer tactic is desired, or it may be free to roam over the entire region. In the following two sections we mainly focus on the control of movement for one swarm.

Since the agents detect a limited sensing radius, we choose to employ two different phases of swarm motion. When there are no targets nearby, the agents should move through the space as quickly and as efficiently as possible, performing a simple flocking movement as legs of a random search. After a signal is sensed via the CUSUM filter, the agents should stop, then slowly move around the area, searching for the exact position of the nearby target. We call these two phases the searching phase and the target-locating phase, respectively. For a general idea of the two types of motion, see Fig. 2.

### 3.1 The Swarming Model

There are a variety of mathematical constructs that lead to agent swarming (see for example (Justh and Krishnaprasad, 2004), (Vicsek et al., 1995), and (Sepulchre et al., 2008)). Here we choose a second-order control algorithm similar to that described in (D’Orsogna et al., 2006) and (Chuang et al., 2007), which has been successfully implemented as a control algorithm for second-order vehicles on real testbeds

(Nguyen et al., 2005; Leung et al., 2007). In this system, each agent of the swarm is subject to self-propulsion and drag, and attractive, repulsive, and velocity alignment forces from each of the other agents. The position  $x_i$  and velocity  $v_i$  of an individual agent  $i$  with mass  $m_i$  in a swarm of  $N$  agents are governed by

$$\frac{dx_i}{dt} = v_i, \quad (10)$$

and

$$m_i \frac{dv_i}{dt} = (\alpha - \beta |v_i|^2) v_i - \nabla U(x_i) + \sum_{j=1}^N C_o (v_j - v_i), \quad (11)$$

where

$$U(x_i) = \sum_{j=1}^N C_r e^{-|x_i - x_j|/l_r} - C_a e^{-|x_i - x_j|/l_a}. \quad (12)$$

$C_r$  and  $l_r$  are the strength and characteristic length of the repulsive force, respectively, and  $C_a$  and  $l_a$  are the corresponding values for the attractive force.  $C_o$  is the velocity alignment coefficient,  $\alpha$  is the self-propulsion coefficient and  $\beta$  is for drag. Depending on these parameters, the swarm can undergo several complex motions (D’Orsogna et al., 2006), two of which are flocking and milling, and in some cases the swarm can alter its motion spontaneously (Kolpas et al., 2007). For our purposes, we simply set these parameters to obtain the type of motion desired.

### 3.2 Searching Phase

In this phase, the agents move together in one direction as a uniformly-spaced group travelling with a fixed velocity. Since the agents know nothing yet about the location of targets, a random search is chosen here. Specifically, we use a Lévy flight, which is optimally efficient under random search conditions (Viswanathan et al., 1999), and is the same movement that some birds employ while flocking and searching for food (Travis, 2007). To accomplish this type of search, we simply command the swarm to turn by a random angle after flocking for some random amount of time. For a Lévy flight, the time interval  $\Delta t$  between two turns follows the heavy-tailed distribution

$$P(\Delta t) \sim \Delta t^{-\mu}, \quad (13)$$

where  $\mu$  is a number satisfying  $1 < \mu < 3$ . The value of  $\mu$  should be chosen optimally according to the scenario in question, as in (Viswanathan et al., 1999). For destructive searching (where targets, once located, are no longer considered valid targets),  $\mu$  should be as

close to 1 as possible. For non-destructive searching (i.e. located targets remain as valid future targets), the optimal  $\mu \sim 2 - 1/[\ln(\lambda/r_s)]^2$ , where  $\lambda$  is the mean distance between targets and  $r_s$  is the sensing radius.

### 3.3 Target Locating Phase

When enough agents agree that a target is nearby (see Section 2.2), the target-locating phase begins. This minimum number of agents is set by the swarm consensus parameter  $p$ , such that the swarm decides to enter this phase when  $p\%$  of the agents or more in the swarm are sensing a target. Once in this phase, we want the agents to move only towards the target, so we remove the velocity alignment force ( $C_o = 0$ ), disable self-propulsion ( $\alpha = 0$ ), and issue a halt command so that all agents begin target-locating with zero velocity. In addition, data from agents within the sensing radius is used to continually estimate the position  $\bar{y}$  of the target (see Section 4), and the agents in the swarm then try to move towards it, thus attracting other agents in the swarm not yet in the sensing radius to move closer to the target as well. To make the agents move towards the target, we add another potential in Eq. 12,

$$U_c = C_c(x_i - \bar{y})^2/2, \quad (14)$$

where  $\bar{y}$  is the estimated position of the target, and  $C_c$  is an adjustable parameter. The full control equations in the target-locating phase therefore become Eq. 10 and

$$m_i \frac{dv_i}{dt} = -\beta |v_i|^2 v_i - \nabla U(x_i), \quad (15)$$

where

$$U(x_i) = \frac{1}{2} C_c (x_i - \bar{y})^2 + \sum_{j=1}^N C_r e^{-|x_i - x_j|/l_r} - C_a e^{-|x_i - x_j|/l_a}. \quad (16)$$

To show that this system converges to a stationary swarm centered on the target, we note that the total energy of the target-locating system,

$$E = \frac{1}{2} \sum_{i=1}^N m_i |v_i|^2 + \sum_{i=1}^N U(x_i), \quad (17)$$

serves as a Lyapunov function, so that the collective tends to minimize it. That is,

$$\dot{E} = -\beta \sum_{i=1}^N |v_i|^4 \leq 0. \quad (18)$$

Hence, velocities will eventually reach zero (due to drag) and the swarm members will spatially re-order themselves so as to minimize the potential energy, forming a regular pattern centered at the target

position. This stationary state serves as a spiral sink, however, so the swarm tends to oscillate about the target position for some amount of time that depends on the value of  $C_c$ , with a high  $C_c$  yielding less oscillation. However, since the potential being minimized now includes a term that is effectively attracting all of the agents towards the center of mass, the swarm will be more compact than it was before the target-locating potential was added, so too large of a  $C_c$  will make the swarm smaller than desired. In practice, we want  $C_c$  just large enough to minimize the oscillations in space without making the swarm get too compact.

## 4 LOCATING TARGETS

During the target-locating phase of motion, all agents of the swarm that are within the sensing radius keep a common register of all of their positions and signal readings made since entering the radius (see ‘‘Threshold Check’’, Section 2.2, above). The agents then use a least-squares algorithm to give an estimate  $\bar{y}$  of where the target is located via

$$\bar{y} = \min_y \sum_{k=1}^{N'} [g(|y - x(t_k)|) - f(t_k)]^2, \quad (19)$$

where  $N'$  is the number of sensor readings in the common register.

Solving this least-squares minimization is straightforward, but certain assumptions for workability and precision are needed. It is assumed that the form of  $g(r)$  is known by the agents for the algorithm to work. For certain classes of targets and scalar fields, we believe this assumption to be fair. For precisely estimating a target’s position, we also assume that only one target is within sensing range, or that target sensing radii do not overlap significantly, so that one target is much closer to the agents than any other target. When the sensing radii are small compared to the average distance between targets, these assumptions should hold true. If, instead they prove to be invalid for the particular system at hand, other methods such as gradient estimation could be used.

If the estimated position of the target stabilizes, it is considered to have been located, and the agents register the position of the target and return to the searching phase: the model signal  $g(r)$  from the registered target will be subtracted from further sensor readings so that it is not detected again, a form of destructive

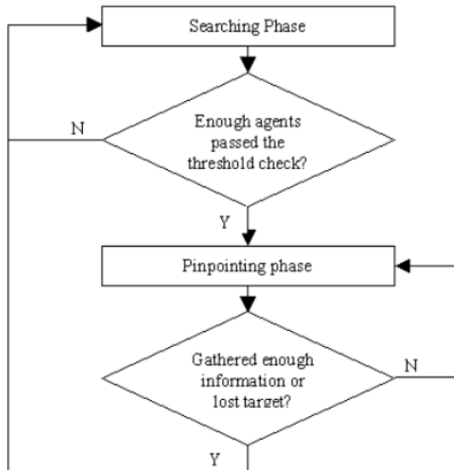


Figure 3: A simple flowchart of the algorithm.

searching. We thus modify Eq. 1 to read:

$$s_i(t_k) = \sum_{j=1}^M g(|y_j - x_i(t_k)|) + n_i(t_k) - \sum_{j=1}^{M'} g(|\bar{y}_j - x_i(t_k)|), \quad (20)$$

where  $M'$  is the total number of registered targets. Note that the positions of these targets may or may not be accurate, due to noise and other errors. If, instead of the estimated target location stabilizing, the agents lose track of the target, they simply return to the searching phase without registering the target. For a general idea of the entire algorithm, see Fig. 3.

## 5 PERFORMANCE EVALUATION

Two main criteria for the evaluation of this algorithm are efficiency and accuracy. These are roughly determined by the two phases: efficiency is mainly related to the searching phase, while accuracy is mainly related to the target-locating phase. To evaluate the performance of the algorithm, we divided the agents into groups and took the following measurements: the average time needed for a swarm to detect and locate a target (Average time), the average distance between the actual and estimated target positions (Average error), and the percentage of registered positions that are not within any actual sensing radius (False registers percentage). Note that false registers are not included in the average error calculation.

We ran computer simulations of the algorithm in a dimensionless 20 by 20 area, with a total of 32 agents

Table 1: Case 1: 20 targets, time limit 50.0. Asterisks denote the use of the divide-and-conquer tactic.

| Swarms | Agents/swarm | Average time | Average error | False reg. |
|--------|--------------|--------------|---------------|------------|
| 1      | 32           | 9.17         | 0.163         | 9.77%      |
| 2*     | 16           | 4.83         | 0.155         | 8.40%      |
| 2      | 16           | 5.45         | 0.159         | 11.90%     |
| 4*     | 8            | 3.15         | 0.158         | 8.68%      |
| 4      | 8            | 3.52         | 0.16          | 10.59%     |
| 8*     | 4            | 2.67         | 0.208         | 9.91%      |
| 8      | 4            | 2.9          | 0.200         | 11.73%     |
| 16*    | 2            | 2.64         | 0.257         | 15.59%     |
| 16     | 2            | 2.64         | 0.253         | 15.17%     |

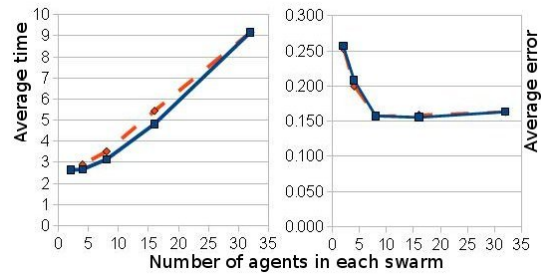


Figure 4: Average detection time (left) and average error (right) as a function of the number of agents in each swarm for case 1 (20 targets and time limit 50.0). The continuous line is for the divide-and-conquer tactic and the dashed line is for the results without divide-and-conquer.

and a number of randomly placed targets each with a dimensionless sensing radius of 1. The signals are Gaussian (as previously described in Section 2), with a peak signal-to-noise ratio of about 10.5 dB. Two cases were considered. In the first case, there were 20 targets and we restricted the duration of the simulation, the main goal being that of measuring efficiency. In the second case, we distributed just 5 targets randomly, and used a much longer time limit, with the main goal of measuring accuracy. In both cases, the simulation ends either when time runs out or when all targets are found. For each case, we performed 100 trials and calculated the average of the measurements.

Since we considered multiple groups of agents, it was important to decide how they must cooperate with one another. We tried two different policies. One was a simple divide-and-conquer tactic where we divide the whole region into sub-regions before the simulation, with each swarm in charge of a single sub-region (Enright et al., 2005; Hsieh et al., 2006), remaining within that area the entire time, and perform-

Table 2: Case 2: 5 targets, time limit 200.0. Asterisks denote the use of the divide-and-conquer tactic.

| Swarms | Agents/swarm | Average time | Average error | False reg. |
|--------|--------------|--------------|---------------|------------|
| 1      | 32           | 45.53        | 0.128         | 10.76%     |
| 2*     | 16           | 25.51        | 0.116         | 8.06%      |
| 2      | 16           | 26.89        | 0.117         | 8.95%      |
| 4*     | 8            | 14.22        | 0.134         | 8.96%      |
| 4      | 8            | 16.64        | 0.118         | 8.79%      |
| 8*     | 4            | 8.35         | 0.161         | 7.24%      |
| 8      | 4            | 10.58        | 0.172         | 8.97%      |
| 16*    | 2            | 8.31         | 0.223         | 11.97%     |
| 16     | 2            | 8.91         | 0.252         | 13.79%     |

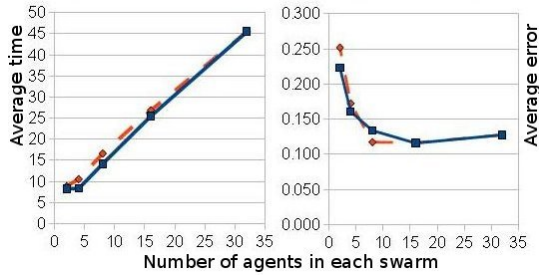


Figure 5: Average detection time (left) and average error (right) as a function of the number of agents in each swarm for case 2 (5 targets and time limit 200.0). The continuous line is for the divide-and-conquer tactic, and the dashed line is for the results without divide-and-conquer.

ing a Lévy flight search pattern confined to its designated area. The other policy allows the swarms to search the entire region independently of one another. In the results, we denoted the use of the divide-and-conquer tactic with an asterisk (\*).

An important factor that influenced our results is the number of groups into which we divided the agents, or equivalently, the number of agents in each swarm. We therefore present the results for several choices of this number. They are in Tables 1 and 2, with the associated plots presented in Figs. 4 and 5.

From the tables and their corresponding plots we see that the number of agents in the swarm works as a balance between accuracy and efficiency. As could have been anticipated, larger swarms give more accurate results (smaller target position error, less false registers), while multiple, smaller swarms make the search more efficient (shorter detection time). To have an acceptably low error and low false register percentage, groups of at least four agents should be used. This is perhaps due to the fact that at least three

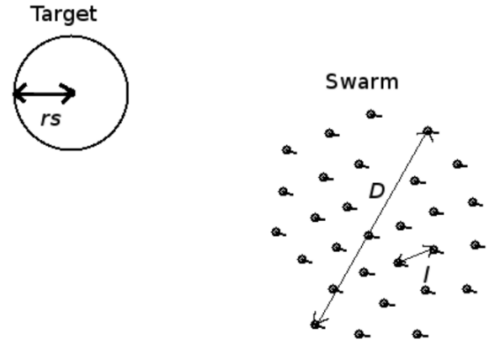


Figure 6: Scales influencing target-locating time: the swarm diameter  $D$ , inter-agent length  $l$ , and sensing radius  $r_s$ .

agents are needed to locate a target, using triangulation. Also, we note that the divide-and-conquer tactic seems to work somewhat better for this scenario.

## 6 SCALING PROPERTIES

Having noted the results above, one may wonder how these are affected by the various scales present in the system, such as the swarm size, distance between agents, target sensing radius, etc. Below we present some arguments for determining optimal search parameters given these scales.

### 6.1 Estimating the Swarm Diameter

We first define a measure for the swarm size, the swarm diameter  $D = \max(|x_i - x_j|)_{i=1}^N$ , where  $N$  is the number of agents in the swarm. Let us also define the inter-agent distance  $l = |x_i - x_j|$  for any two nearest-neighbor agents  $i$  and  $j$  (see Fig. 6).

For the remainder of this section (and for the results in Fig. 7), we choose the parameters of motion so that the system is either in regime VI (catastrophic) or VII (H-stable) as defined in (D’Orsogna et al., 2006), with the swarms flocking naturally in VII, and in VI due to the velocity alignment term  $C_o$  in Eq. 11. Under these regimes,  $D$  and  $l$  stabilize after a transient period, so for the purposes of this section we will consider them to be constant in time. In such a stable swarm, agents are uniformly distributed in space, so that the swarm diameter  $D$  and inter-agent length  $l$  are related geometrically as follows: since the area occupied by a single agent in the swarm is  $A_a \approx \pi l^2/4$  and

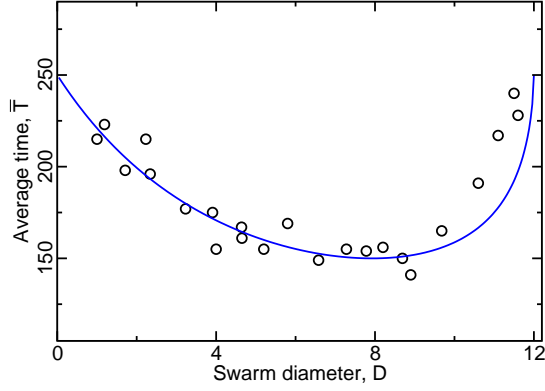


Figure 7: Average time to reach a target  $\bar{T}$  as a function of the swarm diameter  $D$  for  $r_s = 3.0$ . Values of  $D$  were obtained over a range  $C_r = 2.0 - 12.0$ ,  $l_r = 0.2 - 0.7$ , with  $C_a = l_a = 1.0$ . Averaging was carried out over 200 simulated trials, yielding the numerical results (circles); the theoretical results of Eq. 26 with the best fitting  $\tau$  are shown as a line. The number of agents  $N = 16$ , and  $D_{\text{opt}} \approx 8$ .

the total swarm area is  $A_s = \pi D^2/4 \approx NA_a$ , then

$$D \simeq \sqrt{Nl}. \quad (21)$$

Thus,  $D$  scales with  $l$ , and for  $N = 16$  (as used in Fig. 7) we get  $D \simeq 4l$ . Since  $l$  is approximately the distance which minimizes the inter-agent potential of Eq. 12, we can easily adjust the swarm diameter  $D$  by varying the system parameters.

## 6.2 An Upper Bound on the Optimal Swarm Diameter

Consider a setting with one target of sensing radius  $r_s$  and one swarm of diameter  $D$ , as in Fig. 6. We measure the average time to locate the target  $\bar{T}$  by starting the swarm at the center of the search field at time  $t_0$ , placing the target at a random location within the field, allowing the simulation to run until time  $T$  when the target is found, and averaging these  $T$  values over many runs of the simulation. As  $D$  grows, we observe (see Fig. 7) that  $\bar{T}$  decreases until an optimal swarm diameter  $D_{\text{opt}}$  is reached, after which  $\bar{T}$  increases again, growing without bound. We wish to explain this, first by finding an upper bound on  $D_{\text{opt}}$ .

Let us begin by fixing the swarm consensus percentage at  $p = 25\%$ ; i.e., the swarm of agents decides a target is present when 1/4 of the agents or more are within the sensing area of a target,  $A_t = \pi r_s^2$  (see Fig. 8). Clearly, the borderline case between detection and non-detection occurs when the target area is completely subsumed within the swarm area, yet there are only just enough agents (25% of the total) within the

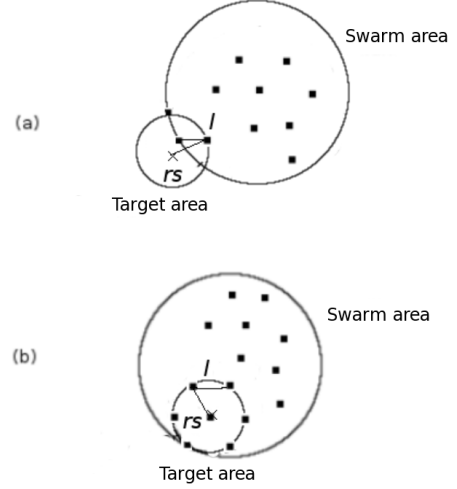


Figure 8: Sensing configurations for the case when 4 or more agents are required to sense the target before it can be detected. (a) Though there is overlap between the swarm and target, too few agents can sense the target for it to be detected. (b) The largest inter-agent distance  $l$  while still allowing for detection,  $l = r_s$ .

target sensing radius to detect it. If we assume a constant density of agents in the swarm, this means that we have detection when the target area is at least  $p\% = 1/4$  of the swarm area. So, it must be the case that

$$D \leq 4r_s, \quad (22)$$

or else the target will not be detected at all. This condition therefore gives an upper bound on  $D_{\text{opt}}$ . Condition (22) can also be written in terms of  $l$ , so that  $l \leq r_s$ ; the borderline case is illustrated in Fig. 8(b). In Fig. 9, snapshots from a simulation show how the swarm flies over the target without being able to detect it in a case when condition (22) is violated.

## 6.3 An Approximation for the Optimal Swarm Diameter

Now that we have an upper bound on  $D_{\text{opt}}$ , we assume that condition (22) is met and look for approximate expressions for  $D_{\text{opt}}$  and  $\bar{T}$ . We note that the area of overlap  $A_o$  between the target and swarm areas, when the centers are separated by a distance  $d$ , is given by

$$A_o = r_s^2 \arccos \left[ \frac{z}{r_s} \right] + \frac{D^2}{4} \arccos \left[ \frac{2(d-z)}{D} \right] - z \sqrt{r_s^2 - z^2} - (d-z) \sqrt{D^2/4 - (d-z)^2}, \quad (23)$$

where

$$z \equiv \frac{r_s^2 - D^2/4 + d^2}{2d}. \quad (24)$$

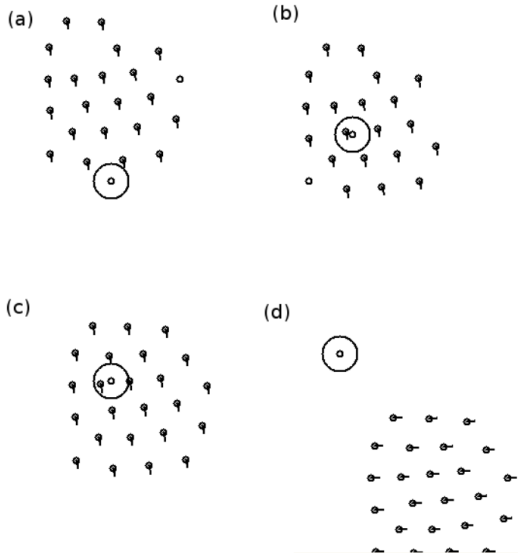


Figure 9: When  $r_s$  is too small compared to  $D$ , the swarm does not detect the target. Snapshots (a)-(d) show the swarm flying over the target without locating it. Here  $N = 24$ ,  $r_s = 1.5$ , required percentage for consensus is  $p = 25\%$ , and  $D$  stabilizes at  $\approx 13.5$ .

Eq. 23 is valid for  $|r_s - D/2| \leq d \leq r_s + D/2$ . Now, as above, we require that  $A_o$  be at least equal to 25% of the swarm area in order for the target to be detected. Thus, we obtain an implicit equation for the maximum separation  $d_{\max}$  between the center of the swarm and the target location such that the target is detected:

$$A_o(r_s, D, d_{\max}) = \pi D^2 / 16. \quad (25)$$

The parameter  $d_{\max}$  will depend therefore upon  $r_s$  and  $D$ . At least in terms of the time spent within the searching phase of the algorithm, the shortest time  $\bar{T}$  until detection ought to occur when, for a given  $r_s$ ,  $D$  is chosen such that  $d_{\max}$  is maximized (see Fig. 10), giving the largest effective target size to hit; hence this  $D$  should be  $D_{\text{opt}}$ . Furthermore, we expect a scaling law such that the time to detection is roughly given by

$$\bar{T} \approx \tau \left[ \frac{A_{\text{field}}}{\pi d_{\max}^2} - 1 \right], \quad (26)$$

where  $\tau$  is a characteristic timescale and  $A_{\text{field}}$  is the total area of the search field.

We have experimentally verified this scaling, with experimental results usually quite close to the theoretical values, as illustrated by the example with  $r_s = 3.0$  in Fig. 7. We note that the actual time to detection is a bit above the theory for  $D > D_{\text{opt}}$ , presumably due to our assumption of constant density in deriving Eq. 25; that is, (especially for large  $D$ ) the area of overlap between target and swarm may be sufficient, but still not

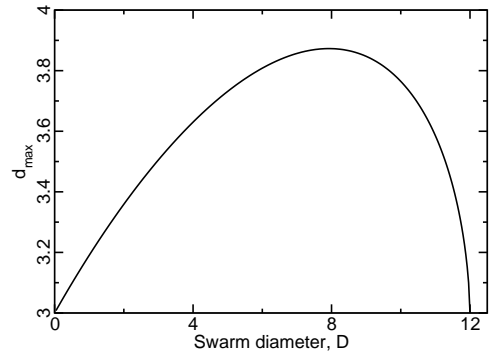


Figure 10: Parameter  $d_{\max}$  versus  $D$  for  $r_s = 3.0$ . Note that  $d_{\max}$  increases at first, as the growing size of the swarm allows it to be further away while still easily satisfying (22). However, after the peak at  $D_{\text{opt}} \approx 8$ , condition (22) becomes the limiting factor, requiring greater overlap between the two areas for detection to occur.

contain at least 25% of the agents, causing the time to detection to be above that expected.

## 7 CONCLUSION

We considered a mine counter-measure scenario using multiple agents that move cooperatively via swarming. The agents use a variety of signal filters to determine when they are within sensing range of a target and to reduce noise for more accurate control and target position estimation. We explored the parameter space through simulations, determining optimal values for some of the search parameters. We derived scaling properties of the system, compared the results with data from the simulations, and found a good analytical-experimental fit.

There are many openings for future research. First, we could use alternative methods in some parts of the algorithm. A potential change is to use a compressed-sensing method (Cai et al., 2008) instead of least-squares for estimating a target's location, which would enable us to find multiple overlapping targets at the same time. Another interesting modification would be to use an anisotropic Lévy search, and take previously covered paths into account. Different scenarios could also be evaluated, which might lead to different results for accuracy and efficiency, or even suggest new algorithms. For example, we could extend the two dimensional problem to 3-D, as would be the case for underwater targets. Or, perhaps the model for the detected signal is unknown, in which case we would employ a different method to estimate the target positions. Finally, apart from

numerical simulations, we plan to do experiments on a real testbed, with small robotic vehicles as agents. This would provide an evaluation of the algorithm in the presence of real sensor noise, which may not be entirely Gaussian in nature.

## ACKNOWLEDGMENTS

The authors would like to thank Alex Chen and Alexander Tartakovsky, whose suggestions on the use of the CUSUM filter were very helpful.

## REFERENCES

- Bopardikar, S. D., Bullo, F., and Hespanha, J. P. (2007). A cooperative homicidal chauffeur game. In *IEEE Conference on Decision and Control*.
- Bullo, F. and Cortes, J. (2005). Adaptive and distributed coordination algorithms for mobile sensing networks. In *Lecture Notes in Control and Information Sciences*. Springer Verlag.
- Burger, M., Landa, Y., Tanushev, N., and Tsai, R. (2008). Discovering point sources in unknown environments. In *The 8th International Workshop on the Algorithmic Foundations of Robotics*.
- Cai, J., Osher, S., and Shen, Z. (2008). Linearized Bregman iterations for compressed sensing. In *UCLA CAM report 08-06*.
- Chen, A., Wittman, T., Tartakovsky, A., and Bertozzi, A. (2009). Image segmentation through efficient boundary sampling. In *8th international conference on Sampling Theory and Applications*.
- Chuang, Y., Huang, Y., D’Orsogna, M., and Bertozzi, A. (2007). Multi-vehicle flocking: Scalability of cooperative control algorithms using pairwise potentials. In *IEEE International Conference on Robotics and Automation*.
- Cook, B., Marthaler, D., Topaz, C., Bertozzi, A., and Kemp, M. (2003). Fractional bandwidth reacquisition algorithms for vsw-mcm. In *Multi-Robot Systems: From Swarms to Intelligent Automata*, volume 2, pages 77–86. Kluwer Academic Publishers, Dordrecht.
- D’Orsogna, M., Chuang, Y., Bertozzi, A., and Chayes, L. (2006). Self-propelled particles with soft-core interactions: Patterns, stability and collapse. In *Physical Review Letters*, 96(10):104302.
- Enright, J., Frazzoli, E., Savla, K. and Bullo, F. (2005). On Multiple UAV Routing with Stochastic Targets: Performance Bounds and Algorithms. In *Proceedings of the AIAA Conference on Guidance, Navigation, and Control*.
- Gao, C., Cortes, J., and Bullo, F. (2008). Notes on averaging over acyclic digraphs and discrete coverage control. In *IEEE Conference on Decision and Control*.
- Hsieh, C., Chuang, Y.-L., Huang, Y., Leung, K., Bertozzi, A., and Frazzoli, E. (2006). An Economical Micro-Car Testbed for Validation of Cooperative Control Strategies. In *Proceedings of the 2006 American Control Conference*, pages 1446–1451.
- Jin, Z. and Bertozzi, A. (2007). Environmental boundary tracking and estimation using multiple autonomous vehicles. In *Proceedings of the 46th IEEE Conference on Decision and Control*.
- Justh, E. and Krishnaprasad, P. (2004). Equilibria and steering laws for planar formations. In *Systems & Control Letters*, 52(1):25–38.
- Leung, K., Hsieh, C., Huang, Y., Joshi, A., Voroninski, V., and Bertozzi, A. (2007). A second generation micro-vehicle testbed for cooperative control and sensing strategie. In *Proceedings of the 2007 American Control Conference*.
- Kolpas, A., Moehlis, J., and Kevrekidis, I. (2007). Coarse-grained analysis of stochasticity-induced switching between collective motion states. In *Proceedings of the National Academy of Sciences USA*, 104:5931–5935.
- Nguyen, B., Yao-Ling, C., Tung, D., Chung, H., Zhipu, J., Ling, S., Marthaler, D., Bertozzi, A., and Murray, R. (2005). Virtual attractive-repulsive potentials for cooperative control of second order dynamic vehicles on the caltech mvwt. In *Proceedings of the American Control Conference*.
- Olfati-Saber, R. (2007). Distributed tracking for mobile sensor networks with information-driven mobility. In *Proceedings of the 2007 American Control Conference*.
- Page, E. (1954). Continuous inspection schemes. In *Biometrika*, 41(1-2):100–115.
- Sepulchre, R., Paley, D., and Leonard, N. (2008). Stabilization of planar collective motion with limited communication. In *IEEE Transactions on Automatic Control*.
- Smith, S. L. and Bullo, F. (2009). The dynamic team forming problem: Throughput and delay for unbiased policies. In *Systems & Control Letters*.
- Travis, J. (2007). Do wandering albatrosses care about math? In *Science*, 318:742–743.
- Vicsek, T., Czirok, A., Ben-Jacob, E., Cohen, I., and Shochet, O. (1995). Novel type of phase transition in a system of self-driven particles. In *Physical Review Letters*, 75:1226–1229.
- Viswanathan, G., Buldyrev, S., Havlin, S., da Luzk, M., Raposok, E., and Stanley, E. (1999). Optimizing the success of random searches. In *Nature*, 401(6756):911–914.